High-sensitivity measurements of the excitation function for Bhabha scattering at MeV energies

H. Tsertos, C. Kozhuharov, P. Armbruster, and P. Kienle
Gesellschaft für Schwerionenforschung (GSI), Planckstrasse 1, D-6100 Darmstadt, Federal Republic of Germany

B. Krusche and K. Schreckenbach
Institut Max von Laue–Paul Langevin (ILL), 156 X Centre de Tri, 38042 Grenoble CEDEX, France
(Received 27 February 1989)

Using a monochromatic e^+ beam scattered on a Be foil and a high-resolution detector device, the excitation function for elastic e^+e^- scattering was measured with a statistical accuracy of 0.25% in 1.4-keV steps in the c.m-energy range between 770 and 840 keV (1.79–1.86 MeV/c^2) at c.m. scattering angles between 80° and 100° (full width at half maximum). Within the experimental sensitivity of 0.5 b eV/sr (c.m.) for the energy-integrated differential cross section no resonances were observed (97% C.L.). From this limit we infer that a hypothetical spinless resonant state should have a width of less than 1.9 meV corresponding to a lifetime limit of 3.5×10^{-13} s. This limit establishes the most stringent bound for new particles in this mass range derived from Bhabha scattering and is independent of assumptions about the internal structure of the hypothetical particles. Less sensitive limits were, in addition, derived around 520-keV c.m. energy ($\sim$1.54 MeV/c^2) from an investigation with a thorium and a Mylar foil as scatterers.

I. INTRODUCTION

Several years ago two independent groups, the Orange and EPOS Collaboration working at GSI in Darmstadt, discovered unexpected narrow positron lines resulting from heavy-ion collisions near the Coulomb barrier.[1–6] Subsequent studies on this field showed pairs of correlated electrons and positrons, which are emitted with similar energies, indicating back-to-back decay.[7,8] Furthermore, high-resolution measurements of positron spectra revealed multiple narrow e^+ lines,[9,10] occurring in a wide range of combined charge Z_u of the two colliding nuclei ($164\le Z_u\le184$) (Ref. 10). In particular, it was found that the energies and widths of the lines do not exhibit any pronounced dependence with respect to the scattering system,[2,6,10] while their production cross sections depend strongly on Z_u: $(d\sigma_{e^+}/d\Omega^*_{\rm ion})\propto Z_u^{22\pm2}$ (Refs. 2 and 10). These experimental facts conclusively exclude the originally proposed mechanism of spontaneous positron creation[11] as origin of these lines. A recent e^+e^- coincidence experiment performed at GSI with a double-Orange β spectrometer[12,13] determined the momentum vectors of positrons and electrons, emitted in heavy-ion collisions, and thus, their opening angle. It indicates a series of e^+e^- sum lines with total energies between 1.5 and 2 MeV, consistent with a two-body decay.[14] The most pronounced sum line appears at a total energy of $\sim$1.83 MeV (Refs. 8 and 14). The origin as well as the production mechanism of the lines still remains a puzzle. They could reflect the existence of a series of e^+e^- resonant states, produced in the Coulomb field of high-Z collision systems,[4,10] which subsequently decay into e^+e^- pairs with lifetime limits of[10]

$$5\times10^{-20}\le\tau^*\le10^{-10}\ \text{s}\ . \tag{1}$$

Stimulated by these observations many theoretical scenarios have recently been put forward,[15,16] postulating the existence of exotic extended objects X with invariant masses in the range (1.5–2.0) MeV/c^2 which undergo a two-body decay: $X\rightarrow e^++e^-$. Their formation in the inverse reaction $e^++e^-\rightarrow X$ requires the invariance under time reversal and laboratory kinetic energies of the incident positrons of the order of $\sim$2 MeV, assuming the electrons to be at rest. This hypothesis, as an explanation of the observed phenomenon, has prompted us to explore the excitation function for elastic e^+e^- scattering (Bhabha scattering) at c.m. energies leading to the corresponding invariant masses of the hypothetical objects. The investigation of this reaction channel is of particular interest, since the sensitivity is basically independent of details of a form factor of the hypothetical resonance (i.e., size, internal structure, etc.). The search for resonant Bhabha scattering in this mass range is, unfortunately, hampered by the relatively weak beams of monoenergetic positrons presently available. In order to achieve sufficient luminosities, the positrons must be scattered on bound electrons. The latter, however, exhibit a momentum distribution due to their localization, which increases with growing atomic binding energy. Thus, the center-of-mass energy available in the scattering process is spread out leading to a Doppler broadening of a narrow resonance. This Doppler broadening becomes less pronounced for low-Z targets (see Fig. 7 below) but is still of the order of 20-30 keV [full width at half maximum (FWHM)] in the laboratory, representing the main experimental limitation in the search for narrow resonances in the excitation function for Bhabha scattering. Consequently, the energy spread of the incident positron beam does not have to be much better than the corresponding Doppler width.

TABLE I. Synopsis of upper limits for resonances in Bhabha scattering obtained from first experiments with various setups.

Experiment performed at	$\sigma_R \Delta E^*_{\text{expt}}$ (b eV)	Res. width Γ^*_R (meV)	Lifetime τ^*_R (s)	Refs.
Murray Hill	$<10^3$	$<2.5\times10^3$	$>2.6\times10^{-16}$	23
Johannesburg[a]	$<2\times10^3$	$<5\times10^3$	$>1.3\times10^{-16}$	24
Stockholm[a]	$<2\times10^3$	$<5\times10^3$	$>1.3\times10^{-16}$	20
Stuttgart	<65	<20	$>3.3\times10^{-14}$	27
Grenoble, Giessen	<65	<20	$>3.3\times10^{-14}$	28 and this work
Groningen	~330		For lifetimes $\sim10^{-13}$ s	29
	20–40		10^{-10}–10^{-12} s	

[a]In these works the observation of a peak structure was claimed.

Because of the large Doppler broadening of high-Z targets (see Fig. 7 below) and the lack of kinematical constraints, first experiments using a continuous spectrum of positrons from β^+ sources scattered on a Th target[17–21] were insensitive to resonance formation.[22] Moreover, a structure observed in these collisions in the positron and electron spectra[17,20,21] cannot have its origin in a new phenomenon,[22] but it can be explained in terms of well-established nuclear processes.[18,19] Among other less sensitive experiments,[23–26] first searches for resonances in scattering of monoenergetic positrons on electrons, bound in Mylar[27,28] and Th (Ref. 28) targets, set upper limits for possible resonant contributions of about 3% of the cross section for Bhabha scattering. A search for long-lived resonances in Bhabha scattering around the invariant mass of 1.8 MeV/c^2 by means of a thick target,[29] was mainly limited by the large background due to the 511-keV annihilation radiation. These first results from Bhabha-scattering experiments, concerning the c.m. upper limits for the energy-integrated total cross section as well as for the intrinsic width and lifetime of a hypothetical spinless resonance, are summarized in Table I. The incident-energy range between ~1 and ~2.5 MeV was covered in these experiments.

Recently we reported the currently most sensitive search for resonances in the excitation function for Bhabha scattering around the invariant mass of 1.8 MeV/c^2, using monoenergetic e^+ beams and a beryllium target as a scatterer.[30] Within a sensitivity of 12.6 b eV (c.m.) for the energy-integrated total cross section no resonant scattering was observed (97% C.L.), measuring the excitation function in beam-energy steps of 5 keV with a statistical accuracy of 0.5% (Ref. 30). In the unitarian limit, the extracted bound for the width and lifetime of a hypothetical spinless resonance amounts to 3.8 meV and 1.7×10^{-13} s, respectively. In contrast with this observation the appearance of a resonance at 1.83 MeV/c^2 with an energy-integrated cross section of ~63 b eV (c.m.) and a width of ~19 meV was reported by a group from Stuttgart at the same time.[31] In this experiment monoenergetic positrons were scattered on a Be foil too. Maier *et al.* conclude in their analysis that the observed resonancelike excess over the smooth Bhabha-scattering cross section is a genuine effect and does not result from statistical or systematic uncertainties.[31] Obviously, our quoted upper limit for the resonance cross section is by a factor of 5 lower than the corresponding cross section of the effect claimed in the Stuttgart experiment (Table II). The probability that both results are consistent is less than 10^{-5}, for an isotropically decaying resonance. Repeating our measurements with improved statistics, we were able to set a new upper limit for resonances around 1.8 MeV/c^2, definitely ruling out the result from Stuttgart.[32] A subsequent search with a sensitivity comparable to that of the Stuttgart experiment was carried out by a Munich group,[33] and in agreement with our results did not show any resonances around 1.8 MeV/c^2 (Table II).

In this paper we describe in detail our high-sensitivity

TABLE II. Recent results from Bhabha-scattering experiments around 1.8 MeV/c^2 using monoenergetic e^+ beams.

Experiment performed at	$\sigma_R \Delta E^*_{\text{expt}}$ (b eV)	Res. width Γ^*_R (meV)	Lifetime τ^*_R (s)	Refs.
Grenoble	No resonance <12.6	<3.8	$>1.7\times10^{-13}$	30
Stuttgart	Resonance $\simeq63$	$\simeq19$	$\simeq3.5\times10^{-14}$	31
Grenoble	No resonance <6.3	<1.9	$>3.5\times10^{-13}$	32 and this work
Munich	No resonance <62	<19	$>3.5\times10^{-14}$	33

measurements of the excitation function for Bhabha scattering, with special emphasis on the experimental methods used. The investigations were mainly concentrated on an invariant mass around 1.8 MeV/c^2, using a clean time-stable monoenergetic positron beam and a metallic Be foil as a target. Our objective was to achieve an experimental sensitivity of a few meV for the width of a narrow resonance, which competes with the most stringent upper bound, derived from a contribution of a hypothetical pointlike particle in this mass range to the precisely measured ($g-2$) factor of the electron.[34]

II. EXPERIMENTAL METHODS

The Bhabha-scattering experiment was carried out at the high-flux reactor of the Institut Laue-Langevin (ILL) in Grenoble using a high-resolution iron-core β spectrometer to provide monoenergetic positrons. Figure 1 shows a general view of the spectrometer BILL and the vertical beam-tube arrangement installed in the reactor.[35] The positron production target consists of a 2.3-mm-thick plate of titanium with an area of 50×130 mm^2 covered in the center by a platinum foil (50×50 mm^2 and 0.25 mm thick). It was exposed to a thermal neutron flux of 3×10^{14} cm^{-2}s^{-1} at an in-pile target position ($\sim$80 cm from the reactor core). The positrons are mainly produced via external pair creation caused by the high-energy γ rays from the ^{48}Ti $(n_{\rm th},\gamma)^{49}$Ti reaction with a cross section of $\sigma_{\rm th}\approx7.8$ b. The titanium plate serves both as (n,γ) source as well as a converter, while the platinum foil contributes weakly to the γ-ray flux but increased significantly the positron yield due to the Z^2 dependence of the $\gamma\rightarrow e^+e^-$ production process. The emerging positrons were momentum analyzed in the 14-m distant spectrometer consisting of two iron-core magnets. Their spectrum, shown in Fig. 2, was measured with a multiwire proportional counter, placed on the focal plane of the spectrometer. It is flat in the energy range of interest, i.e., between 1 and 4 MeV, yielding $\sim1.2\times10^6$ e^+s^{-1} at 2 MeV within the total energy interval of $\sim$30 keV. This positron current follows promptly the neutron flux at the converter site, which is directly proportional to the reactor power. The latter is stable within a few 10^{-3}. For the Bhabha-scattering experiment a beryllium foil (10×100 mm^2 and 4.6 mg/cm^2 thick) was suspended as a scatterer along the focal plane of the spectrometer.

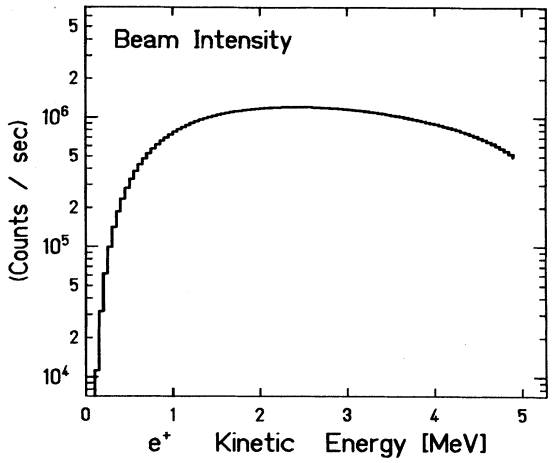

FIG. 2. Incident positron spectrum obtained from a 2.3-mm-thick Ti converter, which was covered in the center with a Pt foil (0.25 mm thick). It was measured using a multiwire proportional counter, placed in the focal plane of the spectrometer. The beam intensity corresponds to a total-momentum interval of $\Delta p/p=1.13\times10^{-2}$, i.e., $\sim$30 keV at a beam energy of 2.3 MeV.

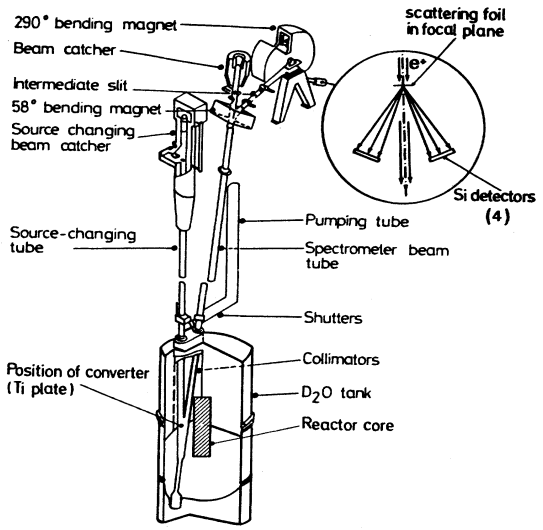

FIG. 1. Scheme of the entire apparatus consisting of a double-focusing β spectrometer and its beam-tube arrangement at the ILL high-flux reactor (Ref. 35). It was used to produce a very clean time-stable monoenergetic positron beam. The momentum-analyzed positrons were finally focused onto a Be foil, placed in the focal plane of the spectrometer (Fig. 3).

Figure 3 illustrates our multiple detector device consisting of two arrays of four high-resolution Si(Li) detectors with an area of 20×20 mm^2 and an effective thickness of 2mm, respectively. They were placed symmetrically relative to the beam direction at a distance of about 85 mm from the Be foil, covering mean scattering angles of $\sim30°$. Bhabha scattering was observed by requiring kinematic coincidences between the scattered positrons and the recoil electrons recorded by two opposite detectors. For normalization purposes, the elastic scattering of positrons at the atomic nucleus (Mott scattering) was in addition recorded in the single spectra of each detector. In order to achieve 100% coincidence efficiency as well as to avoid a sensitivity of the efficiency to slight misalignments, the acceptance angle of one detector row was reduced (about 20%) by apertures, as indicated in Fig. 3(b). Furthermore, the two opposite detector rows were shielded against each other by a low-Z material [Fig. 3(c)], in order to avoid that a Mott-scattered positron, registered in one detector, reaches an opposite detector due to back diffusion. The detectors were cooled by alcohol to approximately $-50\,°$C, achieving an energy and a time resolution better than 7 keV and 4 ns

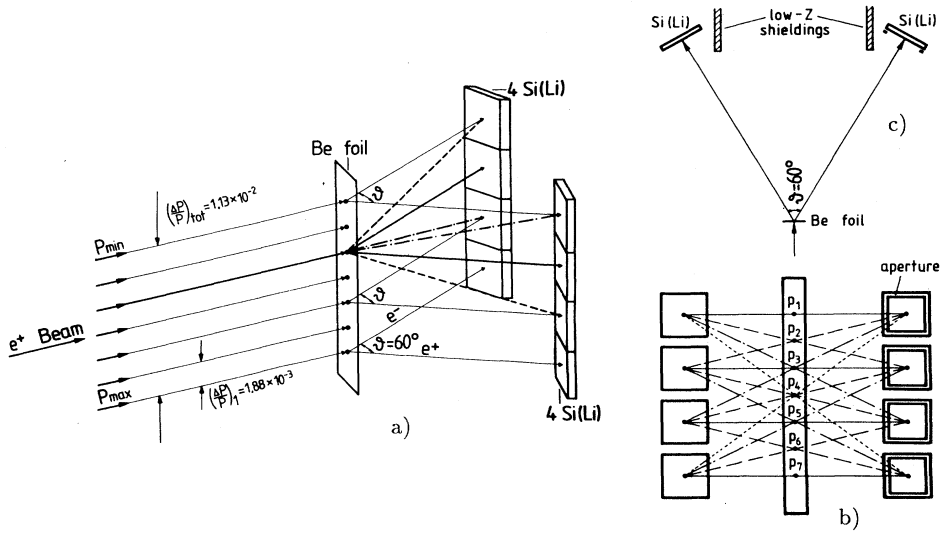

FIG. 3. A perspective [(a)] as well as two projections, perpendicular and parallel to the beam direction [(b) and (c), respectively], of the detection system used to observe Bhabha and Mott scattering. The β spectrometer focuses the e^+ beam onto a Be foil suspended along its focal plane. The scattered particles were detected by two arrays of four high-resolution Si(Li) detectors, placed symmetrically relative to the beam direction at mean angles of about 30°. The total incident momentum bin of $\Delta p/p=1.13\times10^{-2}$, defined by the spectrometer slits, can be subdivided into seven smaller bins of $(\Delta p/p)_i=1.88\times10^{-3}$ by a position determination of the scattering process along the Be foil via kinematic coincidences between the opposite detector pairs [(b)]. Thus, Bhabha scattering is observed within an incident interval of ~5 keV, while the single spectra are measured averaging over the total incident momentum bin (~30 keV).

(FWHM), respectively.

The total incident momentum interval, being limited by a diaphragm in the intermediate image of the spectrometer, amounts to $\Delta p/p=1.13\times10^{-2}$, i.e., ~30 keV at 2.3-MeV beam energy. This relative large incident interval can be subdivided into seven smaller bins by taking advantage of the momentum dispersion of the beam along the focal plane of the spectrometer on the one hand and a position determination of the scattering process in the Be foil by means of kinetic coincidences on the other hand. More accurately, the beam direction together with two opposite detectors, which register a coincident event, define a scattering point on the Be foil. The two detector arrays allow 16 classes of kinematic coincidences which can be related to scattering processes, originating from seven different areas on the Be foil [Fig. 3(b)]. Because of the momentum dispersion of the beam of $\Delta p/p=1.5\times10^{-4}$ per mm, each of these areas with a mean width of 12.5 mm belongs to a momentum bin $(p_1,p_2,\ldots,p_7)$ of $(\Delta p/p)_i=1.88\times10^{-3}$, corresponding to an energy interval of ~5 keV (FWHM) at 2.3 MeV. Thus, seven different, equidistant incident energies are measured simultaneously for Bhabha scattering by each setting of the magnetic field. The single spectra of Mott scattering, however, were measured averaging over the total incident momentum interval.

Our investigations with the Be scatterer were carried out in two independent experiments during two reactor cycles, taking a time of about two weeks per experiment. The excitation function was attained by ten independent runs. For each run the spectrometer field was scanned between 2.13 and 2.38 MeV in steps of 5 keV, with a measuring time of about 40 min per step. Additional runs were also taken in the incident-energy range between 1 and 1.7 MeV using a Th and a Mylar foil as targets. Prior to each run the iron magnets of the spectrometer were demagnetized by repeatedly passing through a number of hysteresis loops with decreasing amplitudes.[35] This procedure, taking a time of 2 h, was necessary for an accurate energy calibration of the spectrometer. The beam energy is reproducible with an accuracy better than 10^{-4}.

All relevant experimental parameters, such as the energies and the time difference of the coincidence events of each opposite detector combination, the energy of the scaled-down single events of each detector, and the setting of the magnetic field of the spectrometer, were stored on magnetic tapes event by event for later analysis. The sum of the Bhabha-scattering events (S_{BE}) was investigated as a function of the magnetic-field setting j in two different ways.

(1) Sum over all coincidence events (C) recorded from the seven detector combinations [Fig. 3(b)] at the same setting j; to control the stability of the device

$$S_{BE}(j\geq1)=[C_1(j)+C_2(j)+\cdots+C_7(j)]\ . \qquad (2)$$

The resulting coincidence spectra are therewith averaged over the total energy interval of the incident beam (~30 keV).

(2) Sum of Bhabha-scattering events corresponding to similar incident positron energies, i.e., taking into account the information of the mean scattering point on the target, as discussed above. In this case the coincidence events from the seven detector combinations were select-

ed at seven different settings of the magnetic field, corresponding to the same incident energy with an interval of ~ 5 keV:

$$S_{\mathrm{BE}}(j \geq 4) = [C_1(j+3) + C_2(j+2) + \cdots + C_7(j-3)] \, . \tag{3}$$

This procedure compensates efficiently long-term instabilities and enables us to distinguish unambiguously between possible systematic errors and resonances, which might occur in the measured excitation function. A systematic error, for instance, appearing for the measuring point j would reveal itself in the excitation function obtained by Eq. (2) as a deviation of a single data point relative to a smooth function. A genuine effect, however, taking place at the incident energy E_{pr} would be registered from all seven detector combinations, which correspond to the same incident energy E_{pr} but to seven different measuring time intervals. For 5-keV measuring steps, it would occur in the excitation function gained by Eq. (3) as a deviation of about six data points, since the experimental resolution for a resonance amounts to ~ 30 keV (see below). We emphasize in this context that no systematic errors were observed from the analysis of the excitation function obtained from Eq. (2). The sum of the Mott-scattering events (S_{ME}) was deduced by adding the single events (S) for each of the seven detector combinations in the same way as being done by the Bhabha-scattering events:

$$S_{\mathrm{ME}}(j \geq 4) = [S_1(j+3) + S_2(j+2) + \cdots + S_7(j-3)] \, . \tag{4}$$

Figure 4 illustrates the quality of the measured sum-coincidence spectra for Bhabha scattering [(a)] and the single spectra for Mott scattering [(b)] gained according to Eqs. (3) and (4), respectively, within the total incident-energy range of observation. For each step the energy (E_{Det}) of the sum coincidence and single events was divided event by event by the actual incident energy (E_{pr}). The latter was accurately determined by the spectrometer calibration (see below). We note here that the measured energies were corrected with respect to the total energy loss in the target (11 and 7 keV for the sum coincidence and single events, respectively). As expected from the kinematics of the two scattering processes, both spectra exhibit sharp peaks centered at one. Their widths of 14 and 25 keV (FWHM), respectively, directly reflect the effective energy spread of the beam and the energy-loss straggling in the target, folded with the detector resolution. They are consistent with the expectation that the effective spread of the beam energy is different for Bhabha and Mott scattering. The 2-mm-thick detectors stop nearly fully the Bhabha-scattered particles (with mean energies of ~ 1.1 MeV), but they act as semi-ΔE detectors for the Mott-scattered positrons (with mean energies of ~ 2.2 MeV), because their range is larger than the effective thickness of the detectors. Therefore, the detection efficiency for a full-energy peak decreases with growing incident energy. This, together with back

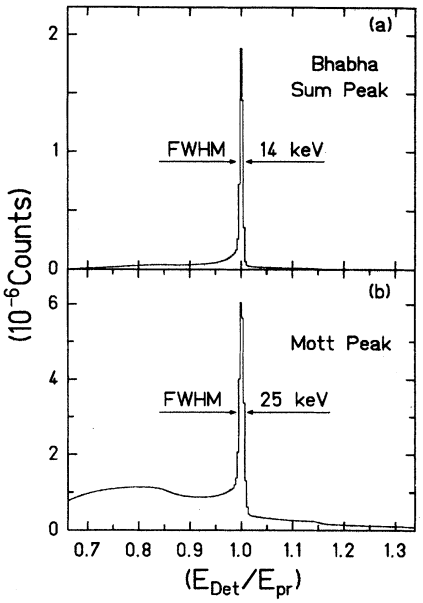

FIG. 4. Energy spectra measured at beam energies between 2.13 and 2.38 MeV in steps of 5 keV for Bhabha as well as for Mott scattering [(a) and (b), respectively]. In the first case, the energies (E_1, E_2) of the coincidence events measured from two opposite detectors in a time interval of about 4 ns (FWHM) were added event by event ($E_{\mathrm{Det}} = E_1 + E_2$), for all possible kinematic coincidence combinations. In the second one, the sum of all single spectra was observed for detector energies E_{Det} greater than about 1500 keV. In both cases, the measured energy E_{Det} is divided event by event by the corresponding actual incident energy E_{pr} for each energy step. The incident energy was determined accurately from the spectrometer setting.

diffusion, causes the broad contribution in the low-energy part of the spectra, distinctly larger for Mott scattering. The decrease of the detection efficiency, however, is a smooth function of the energy and cannot produce any artificial structures. The small contribution in the spectra above the sharp peaks is mainly due to "true" energy summing of a detected positron and a Compton electron, produced by the 511-keV annihilation radiation in the same detector. No other significant background was observed.

The energy calibration of the incident positrons in the focal plane of the spectrometer was gained by inverting the magnetic field and measuring internal conversion electron lines of well-known energy, following the beta decay of ^{116m}In. For each setting of the magnetic field we define as actual incident energy that energy which corresponds to the center of the focal plane, covered by the detector combination No. 4 [see Fig. 3(b)]. The accuracy of the absolute energy scale obtained by this calibration procedure was estimated to be 3 keV. In addition, the pulse height of the detectors was calibrated using the internal-conversion lines from a ^{207}Bi source.

The good energy resolution of the Si(Li) detectors allows an efficient background suppression as well as an accurate determination of the c.m.-scattering angle θ^*, by measuring the energies of the Bhabha-scattered particles

relative to the incident energy. Figure 5 displays such a spectrum which was gained by selecting the Bhabha-scattered events from all detectors using a narrow window around the sum-coincidence peak [see Fig 4(a)]. Their energies were divided event by event by the corresponding kinetic energy of the incident positrons for all energy steps studied. From this, one can deduce the scattering angle θ^* according to the relation

$$\frac{\Delta T}{T_1}=\sin^2\frac{\theta^*}{2}\ , \tag{5}$$

with T_1 being the kinetic energy of the incident positrons, and $\Delta T=T_1-T_1'=T_2'$ the kinetic energy transfer of the incident positrons to the recoil electrons; T_1', T_2' are the kinetic energies of the positrons and electrons after the collision, respectively, undistinguishable in our experiment. (In this work an asterisk refers to quantities in the c.m. system.) This leads to an ambiguity in the determination of the scattering angle θ^* except for the symmetric angle of 90°. The c.m. scattering angle θ^* is connected with the laboratory angle θ by the expression

$$\tan\theta=\frac{1}{\gamma^*}\tan\frac{\theta^*}{2}\ , \tag{6}$$

where

$$\gamma^*=\left[\frac{1}{2}\left[1+\frac{E_1}{m_0}\right]\right]^{1/2}\ . \tag{7}$$

E_1 is the total energy of the incident positron. The angular dependence of the detection efficiency, shown in Fig. 6, was extracted from the spectrum of Fig. 5 by unfolding the angular-dependent cross section for Bhabha scattering [see Eq. (10)]. It exhibits an approximately Gaussian shape with a FWHM of 9° and a mean value centered around ~30°, which corresponds to symmetric Bhabha scattering (90° c.m.) at ~2.2-MeV beam energy. The tails of the curve are mainly due to the beam divergency ($\delta\theta<5°$) and small-angle scattering in the target ($\bar{\theta}\sim4°$ for a coincident event). Note that the energy resolution of the detectors (<7 keV) need not be unfolded because it is negligible compared to the energy interval of ~550 keV (FWHM) covered by the spectrum of Fig. 5. The subtended angular range $80°\le\theta^*\le100°$ (FWHM) in the c.m. system at 2.3 MeV can be subdivided into smaller bins by selecting parts of the measured energy spectrum, as indicated in Fig. 5.

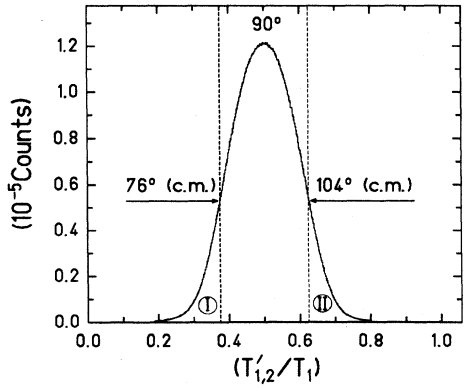

FIG. 5. Sum of the clean Bhabha-scattered events selected event by event from all detectors with a narrow window around the sum-coincidence peak [Fig. 4(a)]. Their energies were also divided event by event by the incident kinetic energy. The distribution obtained reflects the effective angular range of observation, folded with the cross section for Bhabha scattering and with the energy resolution of the detectors. It is centered around 0.5, corresponding to symmetric Bhabha scattering (90° c.m.). By selecting parts of this spectrum, Bhabha scattering can be studied at various scattering angles within the angular range of observation.

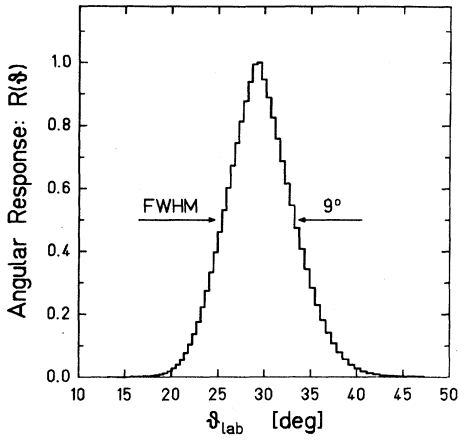

FIG. 6. The effective angular range of observation covered in the laboratory was deduced from the measured energy spectra of the Bhabha-scattered events (Fig. 5) by unfolding the angular-dependent cross section for Bhabha scattering [Eq. (10)]. It exhibits an approximately Gaussian shape, centered around 29.5° with a FWHM of 9°.

The electrons in the low-Z element beryllium were chosen as scatterers to minimize the Doppler broadening of a possible narrow resonance. The condition for the production of a resonance is given by its invariant mass M_R being equal to the total center-of-mass energy E^*:

$$M_R=E^*=2m_0\gamma^*\ . \tag{8}$$

Here it is assumed that the electrons are at rest. However, the motion of an electron with velocity v_e leads to a shift of the center-of-mass energy relative to the case $v_e=0$, which is given by the first-order Doppler effect. In the laboratory frame it can be expressed as

$$\Delta E\simeq\mathbf{v}_e\cdot\mathbf{p}_1\ , \tag{9}$$

with p_1 denoting the momentum of the incident particle. This causes a spread of the center-of-mass energy, thus limiting the peak maximum of a hypothetical narrow resonance relative to the smooth Bhabha-scattering background. Figure 7 demonstrates this effect assuming that a narrow resonance ($\Gamma_R\ll\Delta E$) with $M_R=1.7$ MeV/c^2 is formed in scattering of monoenergetic positrons on bound electrons in Be, Mylar, and Th targets. The distributions, of approximately Lorentzian shape, were gained by a Lorentz transformation of the incident energy taking into account the total Compton profiles of the corre-

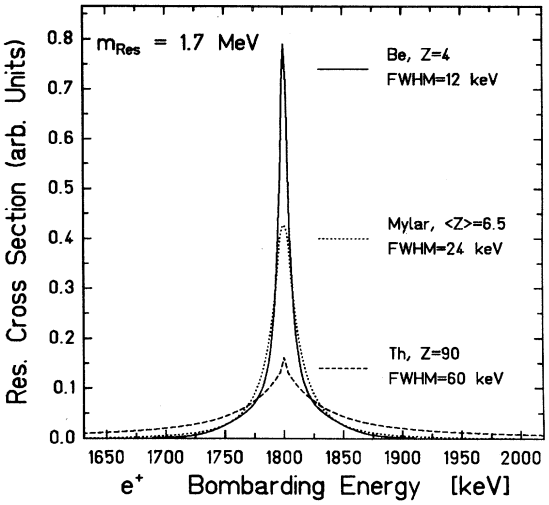

FIG. 7. Calculated Doppler broadening of a hypothetical narrow resonance ($\Gamma_R \ll \Delta E_{\text{expt}}$) at a beam energy of 1.8 MeV, due to the motion of the bound electrons in Be, Mylar $[(C_{10}H_8O_4)_x]$, and Th targets. The distributions of approximately Lorentzian shape were obtained using the total Compton profiles calculated for free atoms (Ref. 36). Their amplitudes are normalized to the total number of the electrons of the corresponding target atom.

sponding target atoms. The electron momentum distributions used here have been calculated theoretically and are available for all free atoms.[36] As can be seen, the Doppler broadening, averaged over all atomic electrons, becomes significantly larger for heavier atoms. For free beryllium atoms, we obtained a Doppler width of $\Delta E \simeq 12$ keV (FWHM) in the laboratory by an incident kinetic energy of 1.8 MeV compared with $\Delta E \geq 60$ keV (FWHM) for a Th atom. Measurements of the total Compton profile for metallic beryllium (polycrystalline) as used in our experiment, however, exhibit a momentum distribution twice as broad.[37] Based on these measured momentum distributions we calculate a value of $\Delta E \simeq 27$ keV (FWHM) for the Doppler broadening at a beam energy of 2.3 MeV. The folding of this Doppler distribution with those obtained for the energy spread of the incident particles (FWHM ~ 5 keV) and from their energy-loss straggling, taken in the half target thickness (FWHM ~ 4 keV), results in an experimental response function for possible resonances having an approximately Lorentzian shape with a FWHM of about 28 keV (~ 7.8 keV in the c.m. system). The latter is proportional to the momentum of the incident positrons [Eq. (9)]. We emphasize in this context that the resolution of the Si(Li) detectors as well as additional broadening *after* the scattering process (about 8 keV for the sum energy of a Bhabha-scattered event) do not enter into the experimental resolution for a resonance in the excitation function.

The differential cross section for Bhabha scattering,[38] which we quote below, is expressed in terms of the total energy ϵ and momentum p of the incident particle in the c.m. system as well as of the c.m.-scattering angle θ^* (Ref. 39):

$$\left[\frac{d\sigma_B}{d\Omega^*}\right] = \frac{r_e^2 m_0^2}{16\epsilon^2}(B_1+B_2+B_3+B_4+B_5) , \tag{10}$$

with

$$B_1 = \frac{(\epsilon^2+p^2)^2}{p^4}\frac{1}{\sin^4(\theta^*/2)} ,$$

$$B_2 = -\frac{8\epsilon^4 - m_0^4}{p^2\epsilon^2}\frac{1}{\sin^2(\theta^*/2)} ,$$

$$B_3 = \frac{12\epsilon^4 + m_0^4}{\epsilon^4} ,$$

$$B_4 = -\frac{4p^2(\epsilon^2+p^2)}{\epsilon^4}\sin^2\frac{\theta^*}{2} ,$$

$$B_5 = \frac{4p^4}{\epsilon^4}\sin^4\frac{\theta^*}{2} ,$$

and

$$\epsilon = \frac{E^*}{2} = (p^2+m_0^2)^{1/2}, \quad r_e = \frac{e^2}{m_0} \simeq 2.82 \text{ fm}, \quad c = 1 .$$

In addition, the differential cross section for Mott scattering is given as a function of the reduced velocity $\beta = (v/c)$ of the incident positrons and their scattering angle θ in the laboratory frame:[40]

$$\left[\frac{d\sigma_M}{d\Omega}\right] = \frac{Z^2e^4}{4m_0^2}\frac{1-\beta^2}{\beta^4}\frac{1}{\sin^4(\theta/2)}Q(\beta,\theta) , \tag{11}$$

where Q denotes the quantum-mechanical correction, replaced by the following approximate formula:[40]

$$Q(\beta,\theta) = 1-\beta^2\sin^2\frac{\theta}{2} \pm \pi\beta\frac{Z}{137}\left[1-\sin\frac{\theta}{2}\right]\sin\frac{\theta}{2} . \tag{12}$$

This formula is valid for $\beta \simeq 1$ if $(Z/137) \leq 0.2$; the plus-minus sign corresponds to scattering of electrons or positions, respectively. For small angles θ, or for the scattering of slow particles by heavy nuclei, it yields $Q \simeq 1$ and, therefore, Eq. (11) coincides with the classical Rutherford cross section.

The expected Bhabha-to-Mott ratio $(N_B/N_M)_{\text{th}}$ can be calculated as

$$\left[\frac{N_B}{N_M}\right]_{\text{th}} = \left[\frac{\Delta E_B}{\Delta E_M}\right]\left[\frac{N_e}{N_K}\right]\left[\frac{\sigma_B(\Delta\Omega_B)}{\sigma_M(\Delta\Omega_M)}\right]\left[\frac{\epsilon_B}{\epsilon_M}\right] , \tag{13}$$

where $(\Delta E_B/\Delta E_M)$ denotes the ratio of the different energy intervals accepted for Bhabha and Mott scattering; (N_e/N_K) means the number of the electrons N_e per atom N_K, (σ_B/σ_M) is the ratio of the cross sections for Bhabha and Mott scattering, respectively, integrated over the corresponding effective solid angles of observation, and (ϵ_B/ϵ_M) is the ratio of the detection efficiency at the Bhabha and Mott energies, respectively, which increases smoothly with the incident energy.

III. RESULTS AND DISCUSSION

Figure 8 displays the counting rate per 5-keV step obtained for Bhabha and Mott scattering [Figs. 8(a) and 8(b), respectively] as a function of the beam energy, for all data taken with the Be target. For each energy step, the sum of the events ($\sim 1.6\times 10^5$ and $\sim 8.0\times 10^5$ for Bhabha and Mott scattering, respectively) were gained from the corresponding energy spectra (see Fig. 4) by an integration of the full-energy peaks using the uniform window: $[0.991 \leq (E_{\rm Det}/E_{\rm Pr}) \leq 1.009]$. With a statistical accuracy of 0.25% and 0.11%, respectively, both excitation functions are smooth, demonstrating the excellent time stability of the e^+ beam. This implies, furthermore, that the systematic errors occurring in our measurements must be significantly lower than the statistical ones. The general features of the measured excitation functions are in agreement with the expected beam-energy dependence of the scattering process according to Eqs. (10) and (11), respectively. The steeper falloff for Mott scattering is due to the smooth decrease of the detection efficiency at the higher e^+ energies, as discussed in the previous section. In accounting for remaining fluctuations in the counting rates, the Bhabha-scattering events were normalized to those obtained by Mott scattering for each measuring point. This is shown in Fig. 9(a) as a function of the beam energy (lower scale) and of the c.m. excitation energy (upper scale). Since the corresponding rate for Mott scattering is by a factor of 5 larger, the statistical uncertainties are mainly determined by the counting rate for Bhabha scattering.

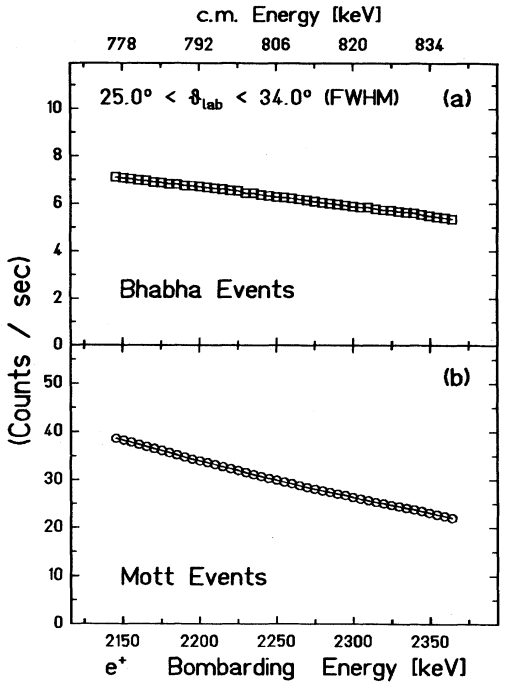

FIG. 8. Total counting rate per 5-keV incident-energy step for Bhabha and Mott scattering [(a) and (b), respectively] as a function of the beam energy. The total measuring time per step amounts to ~400 min.

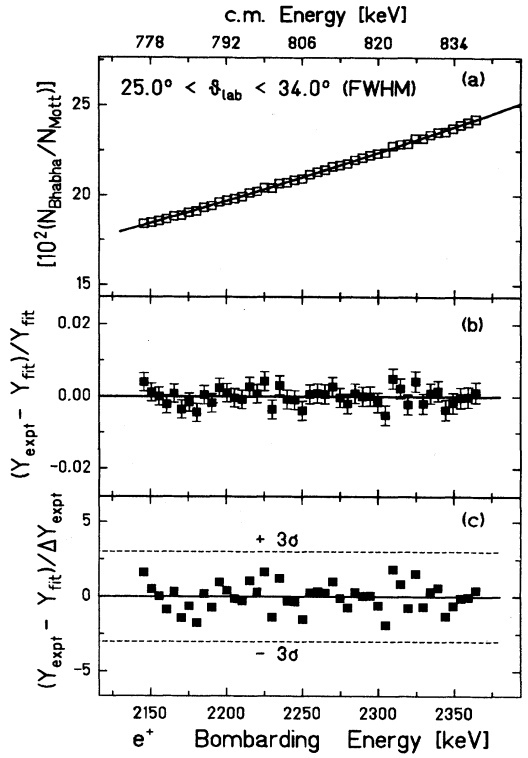

FIG. 9. Measured ratio of Bhabha to Mott scattering obtained from the sum of our data (Fig. 8) as a function of the bombarding energy [(a)]; the corresponding c.m. energy is indicated in the upper scale. The solid line represents a fit of a simple smooth function to the data. The relative as well as the standard deviations from the fitted curve are shown in (b) and (c), respectively.

We now compare the measured ratio with that expected by Eq. (13) at an incident energy of 2.2 MeV. By an integration of the differential cross section for Bhabha and Mott scattering [Eqs. (10) and (11), respectively] we obtain within the full angular range of observation (Fig. 6): $(\sigma_B/\sigma_M) \simeq 0.032$. From a calibration of the detection efficiencies as a function of the incident energy we estimate: $[\epsilon_M(2.2\ {\rm MeV})/\epsilon_B(1.1\ {\rm MeV})] \simeq 14.3\%$; this matches well with calculations showing that the full-energy-peak efficiency of a 2-mm-thick Si(Li) detector only amounts to ~15% at this incident energy.[41] With these values and taking $(\Delta E_B/\Delta E_M) \simeq \frac{5}{25} = 0.2$, $(N_e/N_k) = 4$ we get from Eq. (13): $(N_B/N_M)_{\rm th} = (0.18 \pm 0.03)$. As indicated, the calculated ratio is affected by experimental uncertainties concerning mainly the determination of the detection efficiency at the corresponding Bhabha and Mott energies as well as the effective solid angle for Mott scattering. The estimated value agrees well with the measured ratio of (0.1972 ± 0.0005) at this beam energy. Since our aim, however, was to search for a deviation from a smooth excitation function we did not apply an efficiency correction to the data. For the same reason, the contribution of the random coincidences of about 0.05% was not subtracted from the data, since it was

found to exhibit a smooth beam-energy dependence. Only the incident energy is corrected with respect to the mean energy loss in the target (3.5 keV).

The energy dependence of the measured ratio can perfectly be fitted ($\chi^2/f=1.0$) by a second-order polynomial [Fig. 9(a) solid line]. The relative as well as the standard deviations from the fitted curve are displayed in Figs. 9(b) and 9(c), respectively. As can be seen, no statistically significant deviation from the smooth function was observed on a level of statistical accuracy of 0.25%. Assuming that a resonance is superimposed on the Bhabha-scattering continuum, with a Lorentzian shape and a width fixed to the experimental resolution, its variable maximal height δ relative to the Bhabha cross section can be determined by means of a least-squares-fit procedure applied to the data of Fig. 9(b). The extracted upper limits of δ, depending slightly on the incident energy, are given at the rather conservative 97% confidence level. It should be noted that the choice of a Lorentzian shape, to describe the hypothetical resonance in the laboratory, is justified by the fact that the experimental response is mainly governed by the Doppler effect due to the motion of the electrons. As already mentioned in Sec. II, the resulting distributions (Fig. 7) can better be approximated by a Lorentzian. Control fits assuming a Gaussian shape with the same width, however, yield comparable results. After determination of δ, the following upper limit for the energy-integrated differential cross section of a hypothetical resonance can be derived:

$$\int \frac{d\sigma_R(E^*)}{d\Omega^*} dE^* \leq \delta \left[\frac{d\sigma_B}{d\Omega^*} \right]_{\text{eff}} \Delta E^*_{\text{expt}} \ . \tag{14}$$

The effective Bhabha cross section $(d\sigma_B/d\Omega^*)_{\text{eff}}$ can be deduced by proper weighting of the differential cross section for Bhabha scattering [Eq. (10)] with the angular-dependent detection efficiency $R(\theta^*)$ (Fig. 6) within the full angular range of observation:

$$\left[\frac{d\sigma_B}{d\Omega^*} \right]_{\text{eff}} = \frac{\int_{\theta_1^*}^{\theta_2^*} \frac{d\sigma_B}{d\Omega^*}(\theta^*) R(\theta^*) \sin\theta^* d\theta^*}{\int_{\theta_1^*}^{\theta_2^*} R(\theta^*) \sin\theta^* d\theta^*} \ . \tag{15}$$

The c.m.-energy interval ΔE^*_{expt} is related to the experimental width ΔE_{expt} by the expression

$$\Delta E^*_{\text{expt}} = \frac{m_0}{M_R} \Delta E_{\text{expt}} \ . \tag{16}$$

For instance, at 810-keV c.m. energy ($M_R = 1832\ \text{keV}/c^2$) the following values were obtained: $\delta = 3.5 \times 10^{-3}$, $(d\sigma_B/d\Omega^*)_{\text{eff}} \simeq 18.5$ mb/sr, and $\Delta E^*_{\text{expt}} = 7.8$ keV. Setting these values in (14) we get finally

$$\int \frac{d\sigma_R(E^*)}{d\Omega^*} dE^* \leq 0.5 \ \text{b eV/sr} \ . \tag{17}$$

For a resonance with a cross section σ_R superimposed on the Bhabha-scattering continuum which decays isotropically, the experimental sensitivity to observe it, defined as $\sigma_R/\sqrt{\sigma_B}$, becomes more favorable for

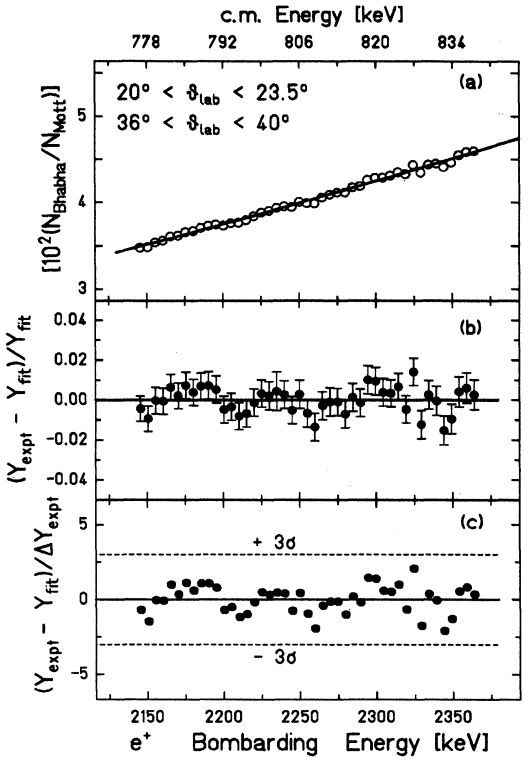

FIG. 10. The same as in Fig. 9, but only Bhabha events corresponding to the small angular window between $20° \leq \theta \leq 23.5°$ and its complementary interval $36° \leq \theta \leq 40°$ are selected. The Bhabha events are normalized to the total Mott events, measured in the full angular range.

scattering angles around the symmetric c.m. angle of 90°. This does not hold, however, in the case of a hypothetical resonance with $J \neq 0$ which can lead to an anisotropic angular distribution of the scattered particles with a minimum at $\theta^* = 90°$, e.g., a resonance with $(d\sigma_R/d\theta^*) \propto \cos^2\theta^*$. According to Reinhardt, Scherdin, Müller, and Greiner[34] the latter rather extreme anisotropy could only take place, if in the initial phase of the collision both leptons are polarized. This requirement, how-

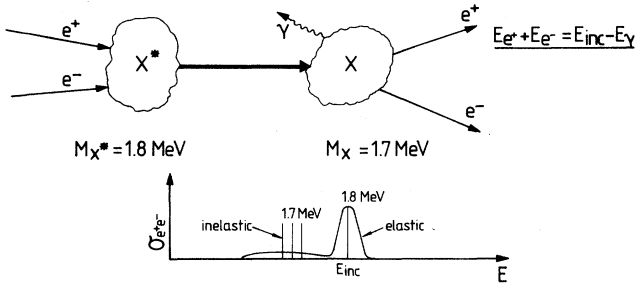

FIG. 11. Schematic depiction of the formation of an excited resonant state X^* with a mass of 1.8 MeV, which undergoes a transition into a state X with a mass of 1.7 MeV by an emission of a real or virtual γ quantum. The state X might eventually decay into an e^+e^- pair whose energy would be about 100 keV lower than that of the incident one.

ever, is not satisfied in our experiments. In order to set a limit even for this case, the effective angular range was restricted to two small complementary angular intervals by means of constraints in the energy spectrum of the Bhabha-scattered particles (Fig. 5). With the window shown in Fig. 5 we were able to select the parts (I) and (II) of this spectrum, which correspond to the scattering-angle ranges between $20° \leq \theta \leq 23.5°$ and $36° \leq \theta \leq 40°$, respectively. The angular range covered in the c.m. system amounts to $66° \leq \theta^* \leq 76°$ (and the corresponding complementary angles). Figure 10 displays the excitation function measured for this reduced angular range. Again, no deviation from a smooth curve was observed with a statistical uncertainty of 0.65%. Using the same procedure as described above an upper limit of 1.3 b eV/sr (c.m.) can be set for the energy-integrated resonance cross section at 810-keV c.m. energy (97% confidence level).

Finally, we addressed ourselves to the question whether our data contain other scattering events apart from the dominant elastic channel of Bhabha scattering. A positive signal would correspond to inelastic channels accounted for by transitions between excited states of an intermediate extended particle. Figure 11 illustrates schematically such a process in which a resonance formed at a higher state with an energy of ~ 1.8 MeV undergoes a transition into a state with an energy of ~ 1.7 MeV by an emission of a γ quantum. This lower state might decay into an e^+e^- pair, the kinetic energy of which would be of about 100 keV lower than the incident one. Our investigation was, therefore, concentrated on such pairs which correspond to the energy range of interest, i.e., on pairs satisfying the condition $(E_{\mathrm{Det}}/E_{\mathrm{pr}}) < 1$ [see Fig. 4(a)]. Obviously, the sensitivity in this case is much higher because only a small fraction of the elastic events, backscattered from the detectors, contribute to the background. However, no evidence for such a process was found, as can be seen from the example given in Fig. 12. In this case we searched in particular for a resonant state with an energy of ~ 1.72 MeV, following the conjecture of Fig. 11. Note that this energy is also suggested from the positron and electron lines observed in the heavy-ion experiments.[9,10,13,14] At each incident-energy step, the scattering events corresponding to the c.m.-energy window of 700±20 keV were selected from the measured coincidence spectra [Fig. 4(a)] and normalized to the total Mott-scattering events. The beam-energy dependence of this ratio does not show any statistically significant deviation from a smooth curve within the statistical errors of 0.9%. From this, an upper limit of 0.15 b eV/sr (c.m.) can be set for the differential cross section of such events (97% C.L.), neglecting the distortion of the scattering kinematics by the emission of the low-energy γ rays.

An upper limit for the intrinsic resonance width, Γ_R^*, can be obtained from the upper bound of the energy-integrated resonance cross section (14) using the relation

$$\int \frac{d\sigma_R(E^*)}{d\Omega^*} dE^* = \frac{\pi}{2} \sigma_R^{\max} \Gamma_R^* \frac{1}{4\pi} . \tag{18}$$

Here it is assumed that the resonance does not interfere with the Bhabha-scattering continuum and that its differential cross section can be described by a Breit-Wigner distribution. This assumption does not substantially influence the final results, since in fact the interference contribution of a narrow resonant state to the Bhabha cross section is found to be negligibly small.[16] The maximal resonance cross section $\sigma_R^{\max}$ is model in-

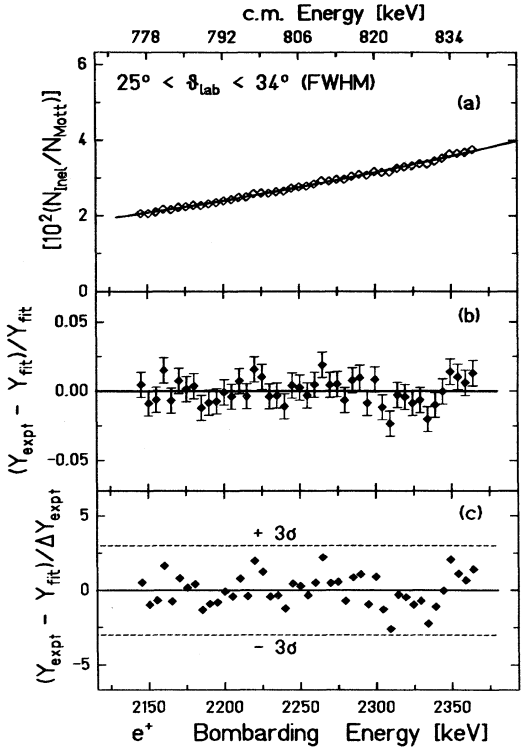

FIG. 12. The same as in Fig. 9, but selecting those events in the sum-coincidence spectra which correspond to a fixed excitation energy of 700±20 keV. For each energy step, this energy window lies below the corresponding elastic sum energy peak when transformed appropriately into the laboratory frame (see Fig. 11). The events obtained are again normalized to the total Mott-scattering events.

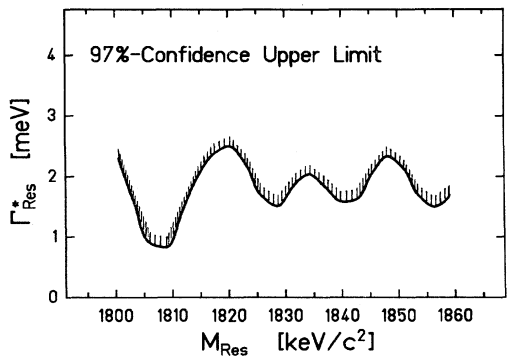

FIG. 13. The upper limits at 97% confidence level to the intrinsic width of a hypothetical spinless resonance as a function of the resonance mass. They were derived from the data of Fig. 9, as described in the text.

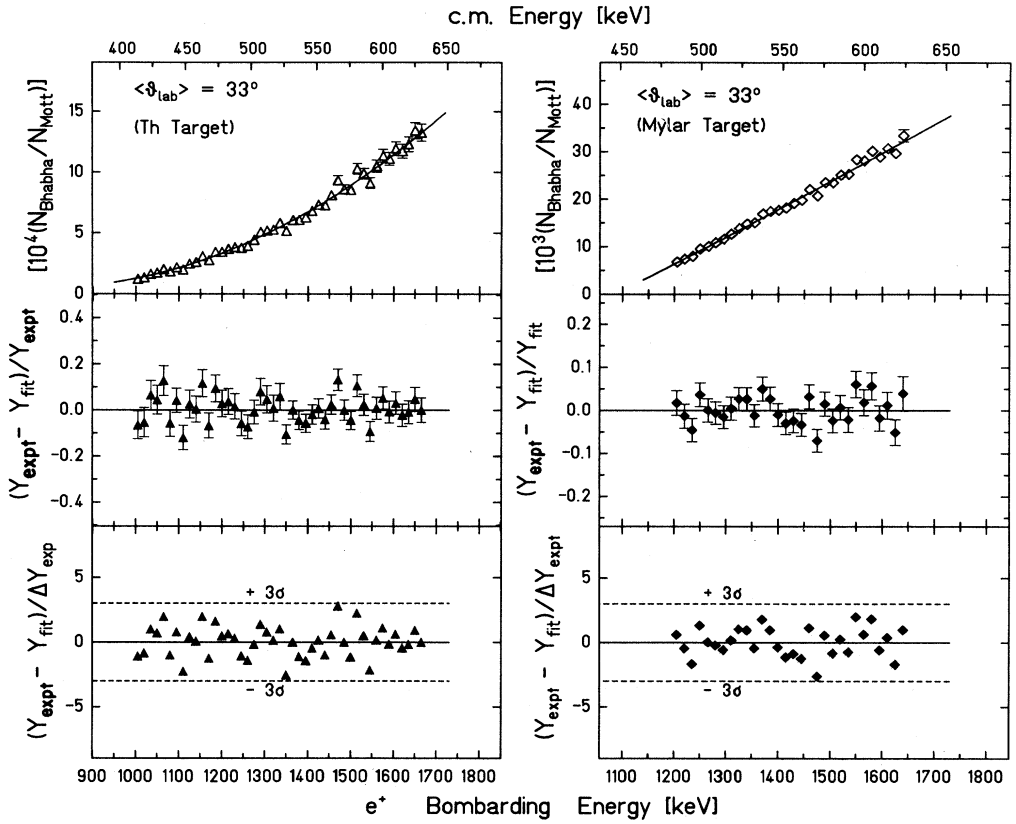

FIG. 14. Measured ratio of Bhabha to Mott scattering obtained from a thorium and a Mylar scatterer (left and right part, respectively) as a function of the bombarding energy. In both cases, the measured excitation function can well be fitted by a simple smooth function (solid lines).

dependent and in the unitarian limit can be expressed as[42]

$$\sigma_R^{\max}=4\pi\lambda\!\!\!^{-2}_R\frac{2J+1}{(2s_1+1)(2s_2+1)}\ , \tag{19}$$

where $\lambda\!\!\!^{-}_R$ denotes the reduced resonance wavelength given by

$$\lambda\!\!\!^{-}_R=\frac{\hbar}{p_1^*}=\frac{2\hbar}{(M_R^2-4m_0^2)^{1/2}}\ , \tag{20}$$

and J the total angular momentum; s_1,s_2 are the spins of the two leptons. We mention, as an example, that Eq. (19) yields $\sigma_R^{\max}\simeq 2116$ b at $M_R=1.832$ MeV/c^2 and $J=0$. The extracted 97%-confidence upper limit of Γ_R^* is displayed in Fig. 13 as a function of the mass of an isotropically decaying resonance ($J=0$). At $M_R=1.832$ MeV/c^2, the limit for the intrinsic width and lifetime amounts to

$$\Gamma_R^*\leq 1.9\ \text{meV}\quad\text{and}\quad\tau^*\geq 3.5\times10^{-13}\ \text{s}\ . \tag{21}$$

This limit represents the currently most sensitive bound for new particles obtained from low-energy Bhabha-scattering experiments. It has already surpassed the sensitivity of the most stringent constraint, deduced from a contribution of a hypothetical pointlike scalar particle to the precisely measured $(g-2)$ factor of the electron.[34] The main advantage of our limit, however, is that is is measured on mass shell and, therefore, independent of assumptions about the internal structure of the hypothetical particles. The bound for lifetimes set by the heavy-ion experiments (1) is therewith improved by several orders of magnitude. However, there is still a lifetime gap between 3.5×10^{-13} s and of 10^{-10} s, not covered by present experiments.

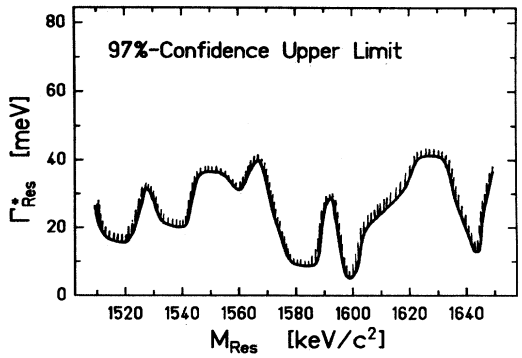

FIG. 15. The same as in Fig. 13, but for the measurement with the Mylar foil (right part of Fig. 14).

In addition, we would like to present briefly the data obtained with lower statistical accuracy using as scatterers metallic thorium (2 mg/cm^2 thick) as well as a 6.4-mg/cm^2 thick Mylar foil [$(C_{10}H_8O_4)_x$]. The incident positron energy was scanned in steps of 15 keV between 1 and 1.65 MeV for the thorium and between 1.2 and 1.65 MeV for the Mylar target, respectively. The energy range around 520 keV (~ 1.54 MeV/c^2) covered in the c.m. system corresponds to the lower energy of the multiple positron and electron lines, found in heavy-ion experiments at GSI (Refs. 9, 10, and 14). In both cases the detectors covered mean laboratory angles of $\sim 33°$ corresponding to symmetric Bhabha scattering at an incident energy of 1.4 MeV. The investigation with the Th target was, in addition, motivated by the results reported elsewhere, in which the observation of a structure in the e^+,e^- spectra resulting from e^++Th collisions is claimed.[17,20,21] According to our above considerations (see Fig. 7), however, thorium with a large Compton profile represents one of the most unfavorable cases in the search for narrow resonances in the excitation function for Bhabha scattering. As can be seen in Fig. 14, both measurements exhibit a smooth excitation function within the statistical uncertainties of about 3%. The 97%-confidence upper limit derived for the intrinsic width of a hypothetical spinless resonance amounts to ~ 80 meV and ~ 20 meV for the thorium and Mylar measurement, respectively. Figure 15 displays the upper limit of Γ_R^* as a function of the resonance mass for the more favorable case of the Mylar measurement.

Although our experimental sensitivity is limited by statistical uncertainties and not yet by systematic errors, the search for lifetimes above 10^{-12} s certainly requires new methods. One such technique might be the well-known shadow method, also proposed in Ref. 29, in which one takes advantage of the fact that a neutral particle formed in e^+e^- scattering may decay after leaving the target, not undergoing energy loss in it. By a conveniently chosen geometry and thickness of the target it could in principle be possible to separate energetically the pairs stemming from the decay of a neutral particle, since the events from nonresonant scattering are shifted to lower energies. Here it is intuitively assumed that the size of the hypothetical particles is sufficiently small so that they would escape undestroyed from the target. This condition, however, is not satisfied for some models, in which exotic particles with very large dimensions are introduced (see Ref. 15). From an experimental point of view the main disadvantage of this method lies in the relatively large background due to energy summing of a positron and a Compton electron from the subsequent 511-keV annihilation radiation. These events lie energetically in the same region in which resonances should occur, thus limiting the experimental sensitivity.[29] Keeping this in mind, experiments with improved setups are now under preparation by us and others[41] aiming at an elimination of this background.

A hypothetical resonance with $J \neq 1$ which decays into an e^+e^- pair can also decay into two photons of equal energy. First searches for correlated narrow two-photon lines from U+Th collisions near the Coulomb barrier have been carried out by Meyerhof and collaborators.[43,44] No structures were seen in these experiments at sum energies in the range in which the e^+e^- lines observed at GSI appear, but a narrow sum γ line at 1062 keV was found.[44] However, the claimed attribution of this observation to the decay of a new neutral intermediate system, which is also responsible for the e^+e^- lines,[44] has not yet been examined rigorously. Recently, other groups have looked for narrow resonances in the two-photon spectrum resulting from positron-electron annihilation in flight, also including the energy region around 1062 keV, in low-[45] and high-resolution[46,47] measurements. Negative results are also reported in these investigations, which are complementary to the Bhabha-scattering experiments. Furthermore, new measurements on Bhabha scattering performed most recently by the Stuttgart group with improved statistics[48] do not corroborate the published results of this group.[31] From the discussion above we conclude that up to now no evidence for an independent signature of process has been found, which could be related to the observed phenomenon at GSI. These features, if also confirmed in the remaining lifetime interval, suggest that the puzzling origin of the e^+e^- lines is closely connected with the domain of heavy-ion physics, involving most probably the strong Coulomb fields occurring in such collisions.[4]

IV. CONCLUSION

We have used a magnetic β spectrometer to produce monoenergetic positrons and a high-resolution multidetector device for a sensitive search for possible resonances in the excitation function for Bhabha scattering around the invariant mass of 1.8 MeV/c^2. With systematic and statistical uncertainties less than 0.25% our data give no evidence for any resonance in this energy range. At 810 keV c.m. energy ($M_R = 1.832$ MeV/c^2), the 97%-confidence upper limit on the energy-integrated resonance cross section is 0.5 b eV/sr (c.m.), corresponding to an intrinsic width and a lifetime of hypothetical spinless resonances of 1.9 meV and 3.5×10^{-13} s, respectively. This limit establishes the most stringent bound for new particles in this mass region derived from Bhabha scattering and is independent of assumptions about their internal structure. Upper limits of $\Gamma_R^* \sim 80$ meV and ~ 20 meV for a Th and Mylar target, respectively, were also obtained around 520 keV c.m. energy (~ 1.54 MeV/c^2) from measurements with lower statistical accuracy. Our results unambiguously exclude all structures reported by other less sensitive experiments,[17,20,21,24,31] clarifying the experimental situation in the search for narrow resonances in e^+e^- scattering at MeV energies. No evidence was also found for possible inelastic channels which would correspond to transitions between excited states of an extended particle prior to the e^+e^- decay.

ACKNOWLEDGMENTS

We would like to thank T. Manning, D. Robinson, and G. Blanc (ILL) for their technical help as well as M.

Richter, H. Essel, H. Sohlbach, and D. Schall (GSI) for their assistance with the data-acquisition and data-analysis system. For fruitful discussions we are indebted to F. Bosch and in particular to W. Koenig as well as to our colleagues from the Frankfurt theory group (W. Greiner, B. Müller, J. Reinhardt, A. Scherdin, and G. Soff). Two of us (H.T.) and (C.K.) acknowledge the hospitality of ILL.

[1]M. Clemente, E. Berdermann, P. Kienle, H. Tsertos, W. Wagner, F. Bosch, C. Kozhuharov, and W. Koenig, Phys. Lett. **137B**, 41 (1984).

[2]H. Tsertos, M. Clemente, E. Berdermann, P. Kienle, W. Wagner, F. Bosch, C. Kozhuharov, and W. Koenig, Phys. Lett. **162B**, 273 (1985).

[3]P. Kienle, Annu. Rev. Nucl. Part. Sci. **36**, 605 (1986).

[4]H. Tsertos, F. Bosch, P. Kienle, W. Koenig, C. Kozhuharov, E. Berdermann, M. Clemente, and W. Wagner, Z. Phys. A **328**, 499 (1987).

[5]J. Schweppe, A. Gruppe, K. Bethge, H. Bokemeyer, T. Cowan, H. Folger, J. S. Greenberg, H. Grein, S. Ito, R. Schule, D. Schwalm, K. E. Stiebing, N. Trautmann, P. Vincent, and M. Waldschimdt, Phys. Rev. Lett. **51**, 2261 (1983).

[6]T. Cowan, H. Backe, M. Bergemann, K. Bethge, H. Bokemeyer, H. Folger, J. S. Greenberg, H. Grein, A. Gruppe, Y. Kido, M. Klüver, D. Schwalm, J. Schweppe, K. E. Stiebing, N. Trautmann, and P. Vincent, Phys. Rev. Lett. **54**, 1761 (1985).

[7]T. Cowan, H. Backe, K. Bethge, H. Bokemeyer, H. Folger, J. S. Greenberg, K. Sakaguchi, D. Schwalm, J. Schweppe, K. E. Stiebing, and P. Vincent, Phys. Rev. Lett. **56**, 444 (1986).

[8]T. Cowan and J. S. Greenberg, in *Physics of Strong Fields,* proceedings of the International Course, Maratea, Italy, 1986, edited by W. Greiner (NATO Advanced Study Institute Series B: Physics, Vol. 153) (Plenum, New York, 1987), p. 111; H. Bokemeyer, *ibid.* p. 195.

[9]H. Tsertos, F. Bosch, P. Kienle, W. Koenig, C. Kozhuharov, E. Berdermann, S. Huchler, and W. Wagner, Z. Phys. A **326**, 235 (1987).

[10]W. Koenig, F. Bosch, P. Kienle, C. Kozhuharov, H. Tsertos, E. Berdermann, S. Huchler, and W. Wagner, Z. Phys. A **328**, 129 (1987).

[11]J Reinhardt, U. Müller, B. Müller, and W. Greiner, Z. Phys. A **303**, 173 (1981).

[12]P. Kienle, Phys. Scr. **T23**, 123 (1988).

[13]E. Berdermann, F. Bosch, P. Kienle, W. Koenig, C. Kozhuharov, H. Tsertos, S. Schuhbeck, S. Huchler, J. Kemmer, and A. Schröter, Nucl. Phys. **A448**, 683c (1988).

[14]W. Koenig, E. Berderman, F. Bosch, S. Huchler, P. Kienle, C. Kozhuharov, A. Schröter, S. Schuhbeck, and H. Tsertos, Phys. Lett. B **218**, 12 (1989).

[15]An excellent report on the present theoretical status as well as many other references relevant to this phenomenon can be found in the recent review article: B Müller, *Atomic Physics of Highly Ionized Atoms,* edited by R. Marrus (Plenum, New York, in press).

[16]In particular with respect to a new phase of QED see D. G. Caldi, A. Chodos, K. Everding, D. A. Owen, and S. Vafaeisefat, in Phys. Rev. D **39**, 1432 (1989), and further references therein.

[17]K. A. Erb, I. Y. Lee, and W. T. Milner, Phys. Lett. B **181**, 52 (1986).

[18]R. Peckhaus, T. W. Elze, T. Happ, and T. Dresel, Phys. Rev. C **36**, 83 (1987).

[19]T. F. Wang, I. Ahmad, S. J. Freedman, R. V. F. Janssens, and J. P. Schiffer, Phys. Rev. C **36**, 2136 (1987).

[20]Chr. Bargholtz, L. Homberg, K. E. Johannsson, D. Liljequist, P.-E. Tegner, L. Bergström, and H. Rubinstein, J. Phys. G **13**, L265 (1987).

[21]M. Sakai, Y. Fujita, M. Imamura, K. Omata, S. Ohya, T. Miura, Phys. Rev. C **38**, 1971 (1988).

[22]H. Tsertos, Phys. Rev. C (to be published).

[23]A. P. Mills, Jr. and J. Levy, Phys. Rev. D **36**, 707 (1987).

[24]U. von Wimmersperg, S. H. Connel, R. F. A. Hoernlé, and E. Sideras-Haddad, Phys. Rev. Lett. **59**, 20 (1987).

[25]J. van Klinken, Phys. Rev. Lett. **60**, 2442 (1988).

[26]U. von Wimmersperg, Phys. Rev. Lett. **60**, 2443 (1988).

[27]K. Maier, W. Bauer, J. Briggmann, H.-D. Carstanjen, W. Decker, J. Diehl, V. Heinemann, J. Major, H.-E. Schaefer, A. Seeger, H. Stoll, P. Wesolowski, E. Widmann, F. Bosch, and W. Koenig, Z. Phys. A **326**, 527 (1987).

[28]P. Kienle, in *Frontiers of Heavy-Ion Physics,* edited by N. Cindro, W. Greiner, and R. Čaplar (World Scientific, Singapore, 1987), p. 363.

[29]J. van Klinken, W. J. Meiring, F. W. N. de Boer, S. J. Schaafsma, V. A. Wichers, S. Y. van der Werf, G. C. Th. Wierda, H. W. Wilschut, and H. Bokemeyer, Phys. Lett. B **205**, 223 (1988).

[30]H. Tsertos, C. Kozhuharov, P. Armbruster, P. Kienle, B. Kruscḧe, and K. Schreckenbach, Phys. Lett. B **207**, 273 (1988).

[31]K. Maier, E. Widmann, W. Bauer, J. Briggmann, H.-D. Carstanjen, W. Decker, J. Diehl, R. Feldmann, B. Keyerleber, J. Major, H.-E. Schaefer, A. Seeger, H. Stoll, F. Bosch, and D. Maden, Z. Phys. A **330**, 173 (1988). (Because of erroneous calculus, the value for the intrinsic resonance width, given in this reference as well as in Ref. 30, is overestimated by a factor of 4. Here we use the corrected values.)

[32]H. Tsertos, C. Kozhuharov, P. Armbruster, P. Kienle, B. Krusche, and K. Schreckenbach, Z. Phys. A **331**, 103 (1988).

[33]E. Lorenz, G. Mageras, U. Stiegler, and I. Huszár, Phys. Lett. B **214**, 10 (1988).

[34]J. Reinhardt, A. Scherdin, B. Müller, and W. Greiner, Z. Phys. A **327**, 367 (1987).

[35]P. Jeuch and W. Mampe, Nucl. Instrum. Methods, **140**, 347 (1977); W. Mampe, K. Schreckenbach, P. Jeuch, B. P. K. Maier, F. Braumandl, J. Larysz, and T. von Egidy, *ibid.* **154**, 127 (1978).

[36]F. Biggs, L. B. Mendelsohn, and J. B. Mann, At. Data Nucl. Data Tables **16**, 201 (1975).

[37]N. K. Hansen, P. Pattison, and J. R. Schneider, Z. Phys. B **35**, 215 (1979); R. Dovesi, C. Pisani, F. Ricca, and C. Roetti, Phys. Rev. B **25**, 3731 (1982).

[38]H. J. Bhabha, Proc. R. Soc. London **A154**, 195 (1936).

[39]L. D. Landau and E. M. Lifschitz, *Lehrbuch der Theoretischen Physik, Band IVa-Relativistische Quantentheorie* (Akademie, Berlin, 1975), p. 344.

[40]R. D. Evans, *The Atomic Nucleus* (McGraw-Hill, New York, 1955), p. 593.

[41]J. van Klinken (private communication).
[42]J. M. Blatt and V. F. Weisskopf, *Theoretical Nuclear Physics* (Wiley, New York, 1952), pp. 406, 423, and 439.
[43]W. E. Meyerhof, J. D. Molitoris, K. Danzmann, D. Spooner, F. S. Stephens, R. M. Diamond, E. M. Beck, A. Schäfer, and B. Müller, Phys. Rev. Lett. **57**, 2139 (1986).
[44]K. Danzmann, W. E. Meyerhof, E. C. Montonegro, Xiang-Yuan Xu, E. Dillard, H. P. Hülskotter, F. S. Stephens, R. M. Diamond, M. A. Deleplanque, A. O. Macchiavelli, J. Schweppe, R. J. McDonald, B. S. Rude, and J. D. Molitoris, Phys. Rev. Lett. **59**, 1885 (1987).
[45]S. H. Connel, R. W. Faerick, R. F. A. Hoernlé, E. Sideras-Haddad, and J. P. F. Sellschop, Phys. Rev. Lett. **60**, 2242 (1988).
[46]M. Minowa, S. Orito, M. Tsuchiaki, and T. Tsukamoto, Phys. Rev. Lett. **62**, 1091 (1989).
[47]J. D. Fox, K. W. Kemper, P. D. Cottle, and R. A. Zingarelli, Phys. Rev. C **39**, 288 (1989).
[48]K. Maier, E. Widmann, W. Bauer, F. Bosch, J. Briggmann, H.-D. Carstanjen, W. Decker, J. Diehl, G. Fabritius, B. Keyerleber, J. Major, H.-E. Schaefer, A. Seeger, and H. Stoll, in *Proceedings of the VII International Conference on Positron Annihilation,* Gent, Belgium, 1988, edited by L. Dorikens-Van Praet, M. Dorikens, and D. Segers (World Scientific, Singapore, 1989); F. Bosch (private communication).